Journal of Al-Azhar University Engineering Sector

Vol. 19, No. 73, October 2024, 1276-1297

SUSTAINABLE COMPOSITES: A STATISTICAL ANALYSIS OF WASTE TIRE RUBBER ADDITION IN POLYESTER-FIBERGLASS PLATES FOR ENHANCED MECHANICAL AND DYNAMIC PROPERTIES

Ahmed. S. AbdelWanees, T. S. Mahmoud, I. M. Ibrahim, Ahmed O. Mosleh

Mechanical Engineering Department - Faculty of Engineering at Shoubra, Benha University, El Sahel, 11614, Cairo, Egypt

***Correspondence:** ahmed.abdallah18@feng.bu.edu.eg

Citation:

A.S.AbdelWanees, T.S.Mahmoud, I.M.Ibrahim, and A.O.Mosleh, "Sustainable Composites: A Statistical Analysis of Waste Tire Rubber Addition in Polyester-Fiberglass Plates for Enhanced Mechanical and Dynamic Properties", Journal of Al-Azhar University Engineering Sector, , vol 19, pp. 1276 - 1297, 2024.

Received: 2024-07-12
Revised: 2024-08-30
Accepted: 2024-09-09
Doi: 10.21608/auej.2024.307165.1690

ABSTRACT

This investigation explores the potential of recycled waste tire rubber to augment the mechanical and dynamic characteristics of eco-friendly polyester-fiberglass composites fabricated using hand lay-up and degassing in a vacuum chamber to eliminate air bubbles. A factorial design methodology was employed to systematically examine the combined influence of mesh size and rubber content on key material properties. Results indicate that both variables, as well as their interactive effects, significantly impact ultimate tensile strength, strain, and impact resistance. Optimal combinations of mesh size and rubber content were identified to achieve the desired mechanical performance levels. While rubber content primarily affected natural frequency, mesh size exhibited a more pronounced influence on damping factor, suggesting the possibility of optimizing damping through careful parameter selection. This study underscores the critical role of mesh size and rubber content in the development of sustainable composites utilizing recycled materials. The factorial design approach effectively captured the complex interactions between these factors, providing valuable insights for tailoring the properties of eco-friendly composites. The findings contribute to the advancement of sustainable materials engineering by demonstrating the feasibility of producing high-performance composites from waste products.

KEYWORDS: Recycling, Waste Tire Rubber Particles, Polyester Composites, Mechanical Behavior, Factorial Design.

المواد المركبة المستدامة: تحليل إحصائي لإضافة مطاط الإطارات المستعملة إلى ألواح البوليستر الزجاجية لتحسين الخصائص الميكانيكية والديناميكية

أحمد سيد عبدالونيس، تامر سمير محمود، إبراهيم موسى إبراهيم، أحمد عمر مصلح

قسم الهندسة الميكانيكية، كلية الهندسة، جامعة بنها، الساحل، 11614، القاهرة، مصر.
***البريد الاليكتروني للباحث الرئيسي :** ahmed.abdallah18@feng.bu.edu.eg

الملخص

يُستكشف في هذا البحث إمكانية تعزيز الخصائص الميكانيكية والديناميكية لمركبات البوليستر والألياف الزجاجية الصديقة للبيئة باستخدام المطاط المعاد تدويره من الإطارات المستعملة.مصنّعة باستخدام الترصيف اليدوي وإزالة الغازات في غرفة تفريغ للقضاء على فقاعات الهواء. تم استخدام منهجية التصميم العاملية لدراسة التأثير المشترك لحجم الجزيئات و محتوى المطاط على خصائص المواد الرئيسية بشكل منهجي .تشير النتائج إلى أن كلا المتغيرين، بالإضافة إلى تأثيراتهما التفاعلية، يؤثران بشكل كبير على القوة الشد والإجهاد ومقاومة الصدم .تم تحديد تركيبات مثلى لحجم ومحتوى المطاط لتحقيق مستويات الأداء الميكانيكي

المطلوبة .بينما أثر محتوى المطاط بشكل أساسي على التردد الطبيعي، فقد أظهر حجم جزيئات المطاط تأثيرًا أكثر وضوحًا على معامل الخمد، مما يشير إلى إمكانية تحسين الخمد من خلال اختيار المعلمات بعناية .يؤكد هذا البحث على الدور الحاسم لحجم ومحتوى المطاط في تطوير المركبات المستدامة باستخدام المواد المعاد تدويرها .نجح نهج التصميم العاملية في التقاط التفاعلات المعقدة بين هذه العوامل، مما قدم رؤى قيمة لتعديل خصائص المركبات الصديقة للبيئة .تساهم النتائج في تقدم هندسة المواد المستدامة من خلال إثبات إمكانية إنتاج مركبات عالية الأداء من المنتجات الثانوية.

الكلمات المفتاحية : إعادة التدوير, جزيئات مطاط الإطارات المستعملة, مركبات البوليستر, السلوك الميكانيكي, و التصميم العاملية.

1. INTRODUCTION

The ever-growing number of discarded tires poses a significant environmental challenge. Stockpiles of waste tires not only occupy valuable space but can also leach harmful chemicals into the surrounding soil and water. Traditional disposal methods like incineration release toxic fumes, further polluting the environment [1].

Researchers are actively exploring innovative solutions to address this growing problem. One promising approach involves incorporating recycled tire rubber particles into building materials. By adding these particles to polyester-fiberglass composites, a widely used material in construction and transportation, researchers aim to create a more sustainable and multifunctional material. Waste tire rubber offers several potential benefits to the composite, including improved impact resistance, sound absorption, and even lower production costs due to the use of recycled materials [2].

Polyester fiberglass composites, often abbreviated as FRP (Fiber Reinforced Polyester), are a popular and versatile class of composite materials prized for their combination of desirable properties. The secret lies in their structure: strong, lightweight fiberglass fibers are embedded within a polyester resin matrix. This marriage of materials grants FRP exceptional strength and stiffness while remaining surprisingly lightweight. Additionally, polyester fiberglass composites boast excellent corrosion resistance, making them ideal for applications exposed to harsh environments. Their good electrical insulation properties are another advantage. These combined qualities have led to widespread use of FRP across various industries, from boat building and transportation to construction and sporting goods [3,4].

Factorial design goes beyond traditional methods by analyzing the influence of multiple variables at once. This powerful approach is especially suited for material engineering, where properties can be affected by factors across different scales. Imagine zooming in from the atomic makeup to the entire manufacturing process – factorial design, with its ability to explore nested factors, allows researchers to see how these various influences interact and impact the final material [5].

Statistical design of experiments (DoE) has been constructed accessible to a wider audience in applied mechanics, particularly those unfamiliar with the concept. Focusing on Response Surface Methodology (RSM) designs like Taguchi, Central Composite, Box-Behnken, and D-optimal, a polymer composites case study is used to compare their effectiveness. The results suggest that exact D-optimal designs can achieve similar accuracy with fewer experiments compared to global D-optimal designs. This highlights the advantages of DoE, the importance of comparing different design options, and provides a framework for selecting the most suitable design for a specific research question [6].

The efficacy of a full factorial design has been assessed in predicting the mechanical properties of polypropylene-kenaf fiber composites. Fabrication involved melt mixing and compression molding. Tensile and flexural strengths were evaluated for composites prepared using a 2x2 factorial design with fiber weight fraction (20/80 and 40/60) and mixing temperature (175°C and 195°C) as variables. The resulting data was used to develop regression equations exploring the influence of these factors. A first-order linear model approximated the response (strength) within the investigated parameter space. This model quantified the individual effects of fiber content and temperature and assessed their interactive influence. The findings demonstrated that the established regression equation, incorporating interaction terms, accurately predicted the mechanical properties within the explored experimental domain [7].

This study proposes a novel composite material incorporating waste tire rubber particles into a polyester matrix reinforced by woven fiberglass. By systematically varying the size and volume percentage of the rubber particles, the investigation delves into their influence on the mechanical and dynamic properties of the composite. A statistical factorial design is implemented to conduct a comprehensive analysis of these variables and to identify the dominant factor affecting each property.

2. Materials and Methods

2.1. Material

The chosen matrix for the composite was a cost-effective and versatile unsaturated polyester resin (UPR) with a density of 1.23 g/cm³ supplied by SUNPOL Company, offering good performance across various composite applications. UPR demonstrates notable mechanical properties, including moderate tensile, flexural, and compressive strengths, as well as moderate impact resistance and good dimensional stability, besides a high degree of reactivity, allowing for rapid curing and solidification when combined with appropriate catalysts and promoters [8].

The recycled rubber particles are based on Styrene-butadiene rubber (SBR) a synthetic elastomer known for its excellent resilience, abrasion resistance, and good tensile strength [9]. When recycled into particle form, it retains many of these properties used in this study originating from Hoppec, an Egyptian supplier. These particles had an average density of 0.4 g/cm3 and were classified within the range of 40 and 20 mesh sizes [10].

Jushi Glass Company's E01 woven fiberglass mat is specifically engineered for the production of high-strength composite materials. Due to its exceptional tensile strength, E01 is well-suited for large-scale structures demanding robust integrity. Furthermore, the material's favorable resin impregnation characteristics and rapid wetting times enable streamlined manufacturing processes with minimal material loss. This combination of excellent mechanical strength and superior acid resistance makes E0-1 a compelling choice for diverse applications such as boat hulls, storage tanks, and chemical processing equipment [11].

2.2. Composite preparation

A hand lay-up technique was employed to fabricate composite laminates. This fundamental and widely used approach offers a versatile and cost-effective method for creating custom composite parts with tailored filler orientations. The process involves the manual application of reinforcement layers onto a mold, followed by their impregnation with resin. This straightforward technique allows for the production of required geometries while enabling good control over fiber placement [12].

A multi-step fabrication process was employed to create composite specimens [13,14]. First, a silicone mold was constructed to ensure the desired final dimensions Two molds were employed for the tensile and impact testing procedures. The tensile mold exhibited dimensions of a= 300mm × b= 170mm × c= 30mm, while the impact mold was more compact, measuring a= 180mm × b= 120mm × c= 30mm shown in **Fig.1** (step 1). The polyester resin was then meticulously measured based on the target volume fraction for precise control over the final resin content (step 2). To eliminate air bubbles detrimental to the composite's integrity, the resin underwent degassing in a vacuum chamber (step 3). For both fiber-reinforced and hybrid-reinforced specimens, the hardener was subsequently added and thoroughly mixed with the degassed resin, following the manufacturer's guidelines (step 4). This mixture then underwent additional degassing to guarantee a homogeneous hardener distribution (step 5). Next, the degassed resin mixture was carefully poured into the mold and allowed to be fully cured at room temperature (step 6).

For hybrid-reinforced specimens, rubber particles were directly incorporated into the resin-hardener mixture before pouring (step 7). In contrast, fiber-reinforced specimens involved cutting fiberglass mats to size and placing them within the mold cavity (step 8).

A fresh resin-hardener mixture (prepared as in step 3) was then applied over the fiberglass mat to ensure proper fiber impregnation (step 9). Rubber particles were directly introduced into the resin-hardener system prepared in step 4. This modified resin matrix was subsequently used for mold casting and curing following the protocol outlined in step 6. Finally, all specimens underwent a final curing step within the mold for approximately two hours (step 10), **Fig. 2** shows a sample of the prepared specimens.

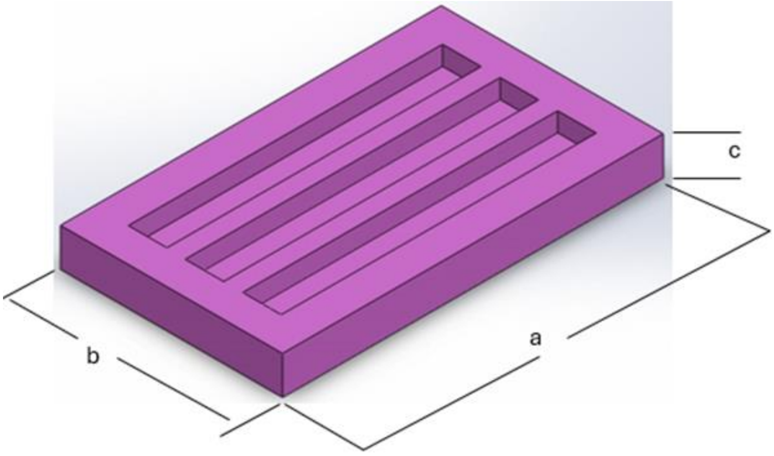

Fig.1: Silicon rubber mold dimensions where, a) length of mold, b) width of mold, and c) thickness of mold.

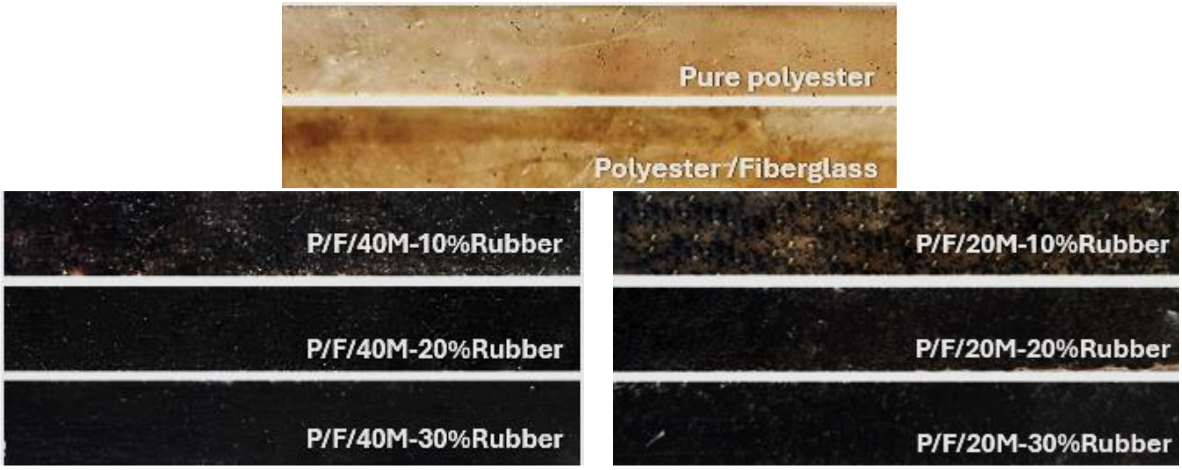

Fig 2: Visual representations of polyester/fiberglass composites enhanced with different proportions of rubber particles with size variation.

2.3. Mechanical testing

The mechanical properties of the composites were evaluated following the standard testing procedures. Tensile testing was conducted according to ASTM D 3039 / D 3039M on a Zwick universal tensile testing machine (Germany) equipped with a 10 kN load cell. The specimens, with dimensions detailed in **Fig. 2-a**, were deformed at a rate of 2 mm/min [15].

Impact resistance was assessed using a JB-300B impact tester (Jinan Shijin Group Corporation) following ASTM D 6110-04. The dimensions of the impact test specimens are presented in **Fig. 2-b** [16].

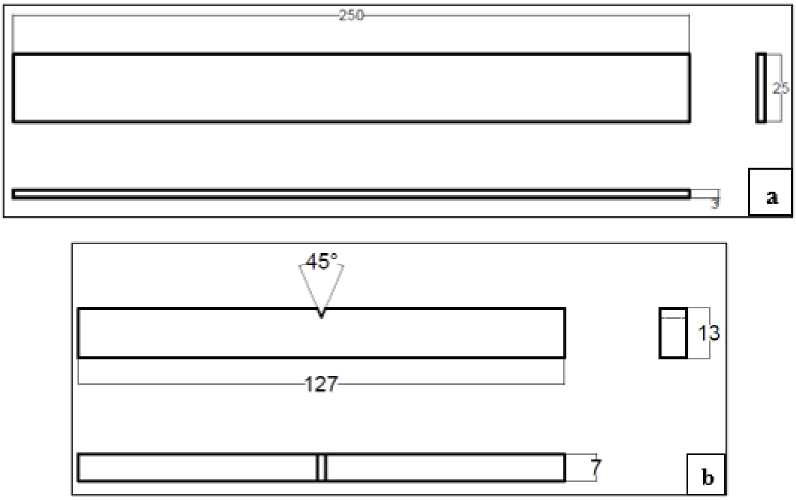

Fig. 2: (a) The dimensions of tensile test specimens in mm, (B) The dimensions of impact test specimens in mm [15,16].

2.4. Free vibration testing

Per ASTM E756-05 [17], a non-destructive free vibration test was employed to assess the inherent stiffness and damping characteristics of the composite materials. This technique evaluates the material's dynamic behavior by measuring its natural frequencies. A rectangular composite beam (210 mm × 24 mm × 4 mm) was fabricated and configured in a cantilever fashion, with one end securely fixed and the other free. To capture the beam's dynamic response during vibration, a B&K model 4507 B accelerometer was attached to the unfixed end. Controlled excitations were delivered to the beam using a B&K model 8206 impulse hammer, and the resulting data was measured by a B&K module 3160-A4/2 impulse data analyzer (as shown in Figure 3). ME'Scope software, dedicated to modal analysis, was then used to process the acquired data and calculate key dynamic parameters such as the frequency response function (FRF), damping ratio, and fundamental frequencies. To guarantee result accuracy and reliability, the free vibration test was repeated five times. The average values from these repetitions were subsequently used to establish correlations between the material properties and the measured dynamic variables.

2.5. Factorial design optimization

Minitab software is utilized with factorial design optimization to efficiently develop and optimize polymer composites containing woven fiberglass and various sizes and volume percentages of waste rubber particles. This technique enables assessing the combined influence of these factors on mechanical properties like tensile strength, strain, impact resistance, damping ratio, and natural frequency. Minitab analysis facilitates the identification of the optimal combination of particle characteristics for achieving desired composite performance.

A multi-criteria approach was used to design the experiment, which means several factors have been considered simultaneously. There were three replicates and 18 total runs. Here's how it's structured in **Table 1**.

Table 1: Factorial design summary layout.

Factors	Mesh Size (mm)		Vol (%)		
Levels	40 (0.42)	20 (0.84)	10%	20%	30%

3. Results and Discussion

This study delves into the influence of waste tire rubber (WTR) on the mechanical properties of composites comprised of polyester resin and fiberglass reinforcements. Specifically, the investigation focuses on WTR particles of two distinct sizes: a finer 40 mesh and a coarser 20 mesh. These WTR particles are incorporated with varying volume fractions within the composite material to assess their impact on the overall mechanical behavior. The chosen volume fractions for the WTR inclusions are 10%, 20%, and 30%, allowing for a comprehensive analysis of how the amount of WTR affects the composite's response to stress. To evaluate the mechanical properties, a series of standardized tests are conducted. The results of these tests, encompassing both traditional mechanical testing methods and free-vibration testing techniques, are compiled and presented in **Table 2** for further analysis. This data will provide valuable insights into how the size and quantity of WTR inclusions influence the strength, flexibility, and overall performance of the polyester-fiberglass composites.

Table 2: The mechanical properties of the manufactured composites.

Mesh Size	Vol%	UTS (MPa)	Strain %	Impact Resistance (Kj/m2)	Natural Frequency (Hz)	Damping Ratio
20	10	8	3.25	35.4	100	0.068
20	20	8.1	3.50	36.7	104	0.064
20	30	12	3.00	35.7	89	0.086
40	10	12	3.50	32.8	108	0.056
40	20	13.5	4.30	41.	131	0.039
40	30	8	3.00	37.3	101	0.035
20	10	7	3.75	36.8	98	0.055
20	20	8.2	3.75	37.4	104	0.042
20	30	10	3.00	34.5	88	0.088
40	10	13	3.50	31.8	110	0.043
40	20	13.4	3.90	42.3	134	0.039
40	30	6.3	2.75	36.5	104	0.044
20	10	8	4.25	34.2	101	0.078
20	20	8.1	3.50	35.9	106	0.086
20	30	13	3.50	36.9	90	0.083
40	10	13	3.50	33.9	106	0.069
40	20	13.6	4.10	39.8	129	0.033
40	30	7	2.50	38.1	98	0.066

3.1. Ultimate tensile strength

Previous studies have established that rubber generally possesses lower inherent tensile strength compared to fiberglass and polyester [18]. Consequently, the addition of rubber particles can potentially weaken the overall composite structure. This weakening effect is likely due to the disruption of the stress transfer mechanism between the strong fiberglass fibers and the polyester matrix caused by the rubber particles. This disruption hinders efficient load distribution within the composite, potentially leading to premature failure under excessive stress [19].

An interesting trend emerged regarding the impact of rubber content on tensile strength. adding rubber particles of different sizes affects the tensile strength of fiberglass-polyester composites. While a small amount of rubber (up to 20%) can improve strength in some cases, a larger amount (30%) generally weakens the composite. This weakening is likely due to rubber particles disrupting the transfer of stress between the fibers and the matrix.

Mesh size also plays a role. larger mesh (M20) seems better for higher rubber content (30%) as it may allow for better dispersion and mitigate the negative impact on stress transfer. However, even with larger mesh, a very high rubber content (30%) can significantly reduce strength. This suggests there might be an optimal balance between rubber content and mesh size for maximizing tensile strength.

3.2. Strain to failure

The addition of rubber particles exhibited a decreasing trend in strain values, particularly for the larger 20 mesh particles as their volume fraction increased. This phenomenon can likely be attributed to the accumulation of these larger particles at higher volume contents, hindering proper adhesion between composite layers. Interestingly, the incorporation of smaller 40 mesh rubber particles was the highest strain observed at a volume fraction of 20%. However, strain values began to decrease at a 30% volume fraction.

3.3. Impact resistance

This study explores the impact of incorporating rubber particles of varying sizes and volume fractions on the impact resistance of polyester/fiberglass (P/F) composites. At a 10% rubber loading level, both M20 and M40 mesh-size composites exhibit a modest enhancement in impact strength. This improvement can be attributed to the elastomeric properties of rubber, which facilitates energy dissipation through mechanisms like reduced stress concentration within the stiffer polyester and glass fiber components, and mitigation of microcrack propagation via bridging or deflection by the rubber particles [20].

However, this trend deviates from higher rubber contents (20% and 30%). The M20 composites display a slight decrease in impact strength (35.4, 36.7, and 35.7 KJ/m^2, respectively) with increasing rubber content. This phenomenon is potentially caused by the enlargement of voids within the composite. Weakening of the interface between the rubber particles and the matrix due to the increased rubber volume fraction creates potential sites for crack initiation under impact loading.

The M40 composites exhibit a more pronounced effect. While the 10% and 20% rubberized composites show significant improvements in impact strength (32.8 and 41 KJ/m^2, respectively), the 30% composite experiences a reduction (37.3 KJ/m^2). This suggests a potential interaction between mesh size and the negative effects of high rubber content. A larger mesh size (M20) might lead to a less uniform distribution of rubber particles, introducing more prominent weak zones within the composite structure.

3.4. Dynamic behavior characterization.

Measuring the damping ratio and natural frequency is crucial for understanding the dynamic behavior of polyester composites reinforced with rubber particles and woven fiberglass mats. The damping ratio quantifies the material's ability to dissipate vibrational energy, which is vital for applications where noise reduction and vibration control are critical. A higher damping ratio signifies greater energy absorption, leading to reduced noise and vibration during operation.

Natural frequency, on the other hand, represents the inherent frequency at which the composite freely vibrates. This knowledge is essential to avoid resonance scenarios where external vibrations can significantly amplify, potentially leading to structural failure. By measuring both damping ratio and natural frequency, researchers can optimize the composite's design to achieve the desired balance between vibration mitigation and structural integrity for specific applications [21].

Furthermore, the inclusion of rubber consistently yielded composites with low natural frequencies. This aligns with the inherent properties of the materials. Rubber exhibits greater elasticity, leading to a reduction in composite stiffness. The extent of this decrease appears to be directly proportional to the rubber content. A higher rubber concentration (30%) resulted in a more pronounced decrease in natural frequency (e.g., 88.5 Hz for P/F/M20_30%) compared to a lower concentration (10%, e.g., 99.6 Hz for P/F/M10_20).

The influence of mesh size on natural frequency was inconclusive. At 10% rubber content, the sample with a smaller mesh size (40 mesh, 109.4 Hz) displayed a higher frequency compared to the one with a larger mesh size (20 mesh, 99.6 Hz).

The analysis of the damping ratio reveals several key trends. The inclusion of rubber particularly at higher volume fractions (30%), especially with 20 mesh size enhanced the damping ratio. This implies that adding rubber improves vibration absorption. The effect of mesh size on damping ratio is less apparent, with M40_30% having the lowest value. Interestingly, P/F/M40_20% appears as an outlier, exhibiting the highest natural frequency along with a moderate damping ratio. This suggests a potential synergistic effect between the 20% rubber content and the 40 mesh. The mean values of the tested mechanical properties are shown in **Table 3.**

Table 3: The central tendency of the data obtained from the mechanical properties' evaluations

Composite	UTS (MPa)	Strain %	Impact Resistance (Kj/m2)	Natural Frequency (Hz)	Damping Ratio
P/F /M20_10% Rubber	7.6	3.75	35.4	99.6	0.068
P/F /M20_20% Rubber	8.1	3.58	36.7	104.1	0.064
P/F /M20_30% Rubber	11.8	3.16	35.7	88.5	0.086
P/F /M40_10% Rubber	12.8	3.45	32.8	109.4	0.056
P/F /M40_20% Rubber	13.5	4.02	41.0	132.1	0.039
P/F /M40_30% Rubber	7.1	2.74	37.3	100.9	0.035

4. Multilevel Factorial Design Optimization

The development of new materials with specific properties is crucial for advancements in engineering. Material engineers achieve this by carefully controlling a material's makeup, processing, and external influences. However, these factors often interact in complex ways, making it difficult to understand their individual effects. This is where multilevel factorial design becomes a powerful tool [22].

Multilevel factorial design allows researchers to study the impact of multiple factors simultaneously, unlike traditional methods that focus on one factor at a time. It goes a step further by incorporating nested factors, revealing how the effect of one factor can change depending on another. This is particularly useful in material engineering, where properties are influenced by factors at various scales, from the atomic level of the material to the large-scale processing techniques used to create it. In this study, this approach will be used to understand how the size and amount of rubber particles affect a composite's mechanical and dynamic properties, such as strength, flexibility, and vibration behavior [23].

4.1. Analysis of factorial design

Cracking the code of multi-factor experiments lies in analyzing factorial designs. This involves meticulously dissecting the data to uncover hidden patterns and relationships. Statistical techniques help us shift through the results, identifying how individual factors and their interactions influence the outcome (response variable). Not only can we determine if each factor has a significant effect, but also how they work together, potentially creating even more complex influences. Ultimately, this analysis aims to provide a clear understanding of how these factors combine to shape the final result [24].

Our analysis reveals a Variance Inflation Factor (VIF) close to 1, This finding suggests a minimal degree of multicollinearity between the focal independent variable and the other independent variables included in the model. Consequently, the variance of the estimated coefficient for the focal variable remains uninhibited. This translates to enhanced reliability and interpretability of the coefficient estimates, ultimately leading to a clearer understanding of the focal variable's isolated effect on the dependent variable.

4.2. Analysis of ultimate tensile strength

A factorial experiment was designed to assess the independent and interactive effects of two factors, Mesh Size and Vol%, on the response variable. Analysis of variance (ANOVA) in **Table 4** revealed a statistically significant model effect (p-value). This indicates that at least one of the factors (Mesh Size, Vol%, or their interaction) has a significant impact on the response variable.

Table 4. ANOVA of ultimate tensile strength.

Analysis of Variance					
Source	DF	Adj SS	Adj MS	F-Value	P-Value
Model	5	118.164	23.6329	37.88	0
Linear	3	23.001	7.667	12.29	0.001
Mesh Size	1	16.82	16.82	26.96	0
Vol%	2	6.181	3.0906	4.95	0.027
2-Way Interactions	2	95.163	47.5817	76.27	0
Mesh Size*Vol%	2	95.163	47.5817	76.27	0
Error	12	7.487	0.6239		
Total	17	125.651			

The low p-value (0.000) suggests the model effectively explains a substantial portion of the variation observed in the response variable. Furthermore, the high F-value (76.22) provides strong evidence that the interaction of mesh size and vol% significantly influences the response variable.

Fig. 4-a reveals that mesh size and its interaction with Vol% exert the most significant influence. Figure 3-b displays the normality plot. While some data points deviate from the straight line, particularly at the edges (tails), this doesn't necessarily imply a significant departure from normality.

The histogram in **Fig. 4-b** portrays the frequency distribution of the residuals. A bell-shaped curve centered around zero would be indicative of normality. The absence of any concerning trends or patterns in the versus plot (**Fig. 4-b**) is encouraging, as it suggests no correlation between the order in which the data was collected and the residuals.

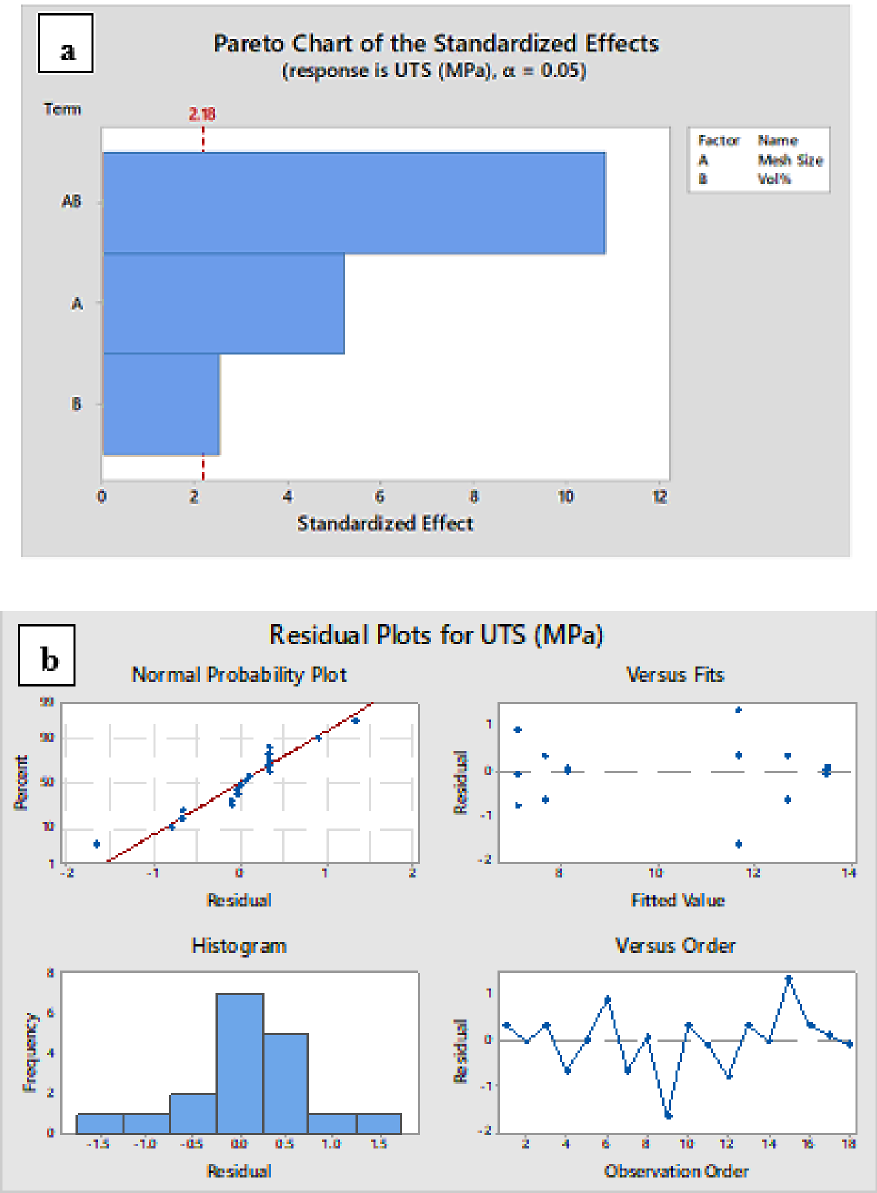

Fig. 4: (a) Pareto Chart of Ultimate Tensile Strength, (b) Residual Plots of Ultimate Tensile Strength.

The results shown in **Fig. 5-a** and **5-b** indicate a positive correlation between decreasing mesh size and UTS (MPa). This suggests that finer meshes generally lead to higher ultimate tensile strength. Conversely, a negative coefficient would imply that UTS (MPa) decreases as mesh size increases. In other words, mesh size has a significant influence on UTS. However, when we consider the combined effect with a specific volume fraction (e.g., 30%), the overall increase in UTS (MPa) might be mitigated or even reversed due to these opposing trends.

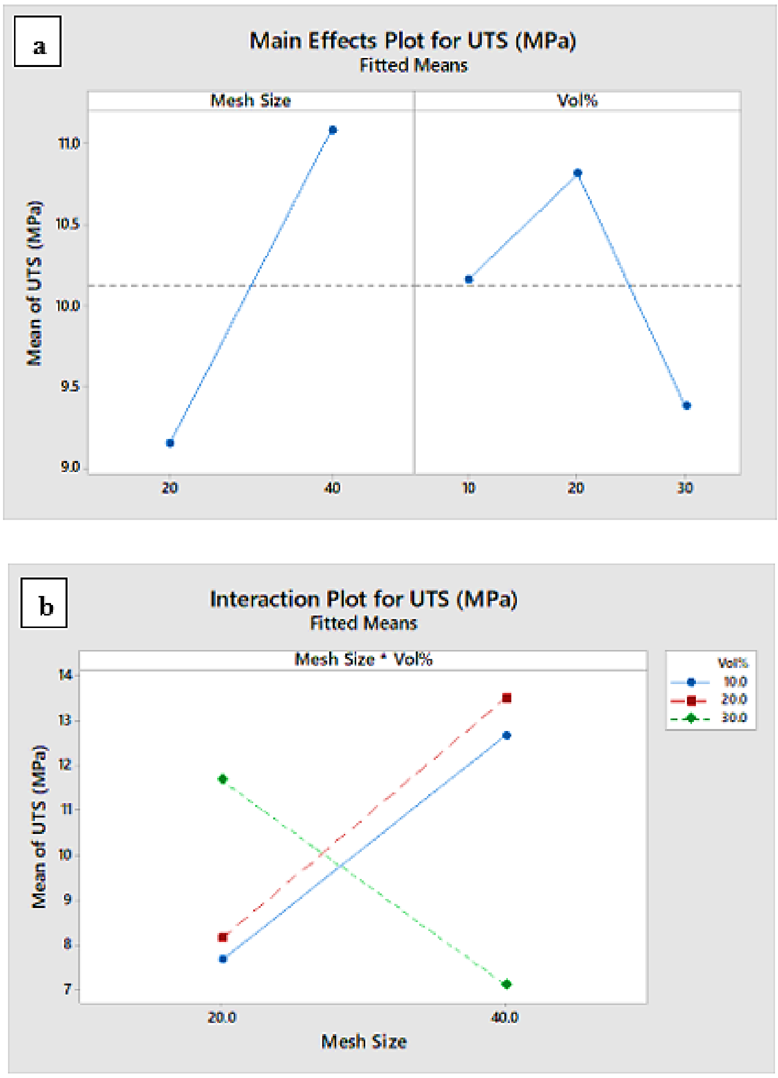

Fig. 5: (a) Main effects plot for ultimate tensile strength, (b) Interaction plot for ultimate tensile strength.

4.3. Analysis of strain

Table 5 tabulated the ANOVA analysis of the strain of the investigated composites. The model has a statistically significant impact on the strain response variable (p-value < 0.05). This implies that one or more of the investigated factors, including mesh size, volume percent, and their interaction, significantly affect the response variable), the F-value in the same table of vol% with zero value of p-value suggests that this factor has a strong influence.

Table 5: ANOVA of strain

Analysis of Variance					
Source	DF	Adj SS	Adj MS	F-Value	P-Value
Model	5	3.29613	0.65923	8.65	0.001
Linear	3	2.54273	0.84758	11.12	0.001
Mesh Size	1	0.01384	0.01384	0.18	0.678
Vol%	2	2.52889	1.26445	16.58	0
2-Way Interactions	2	0.75341	0.3767	4.94	0.027
Mesh Size*Vol%	2	0.75341	0.3767	4.94	0.027
Error	12	0.91494	0.07624		
Total	17	4.21107			

Analysis of **Fig.6-a** reveals important factors influencing the response variable. Vol% and its interaction with mesh size appear to have the strongest impact. This is further supported by the model's explanatory power, suggesting a significant portion of the response variable's variation can be attributed to this interaction. In other words, the combined effect of Vol% and mesh size seems to be more influential than their individual contributions.

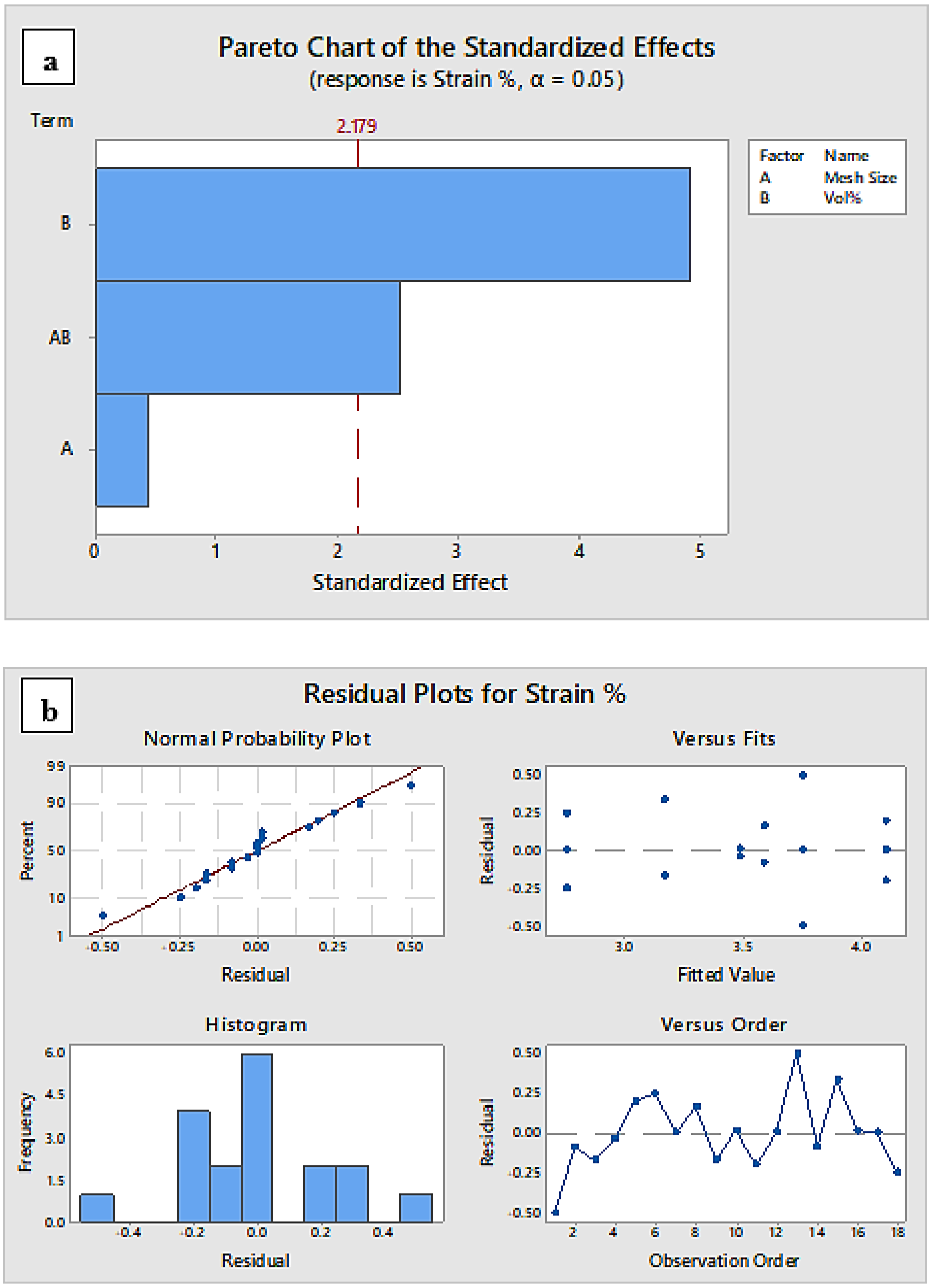

Fig. 6: (a) Pareto chart of strain, (b) Residual plots of strain.

The residual plots for strain in **Fig.6-b** reveal potential areas for model refinement. The normality plot suggests exploring transformations or alternative error models. The histogram's leftward skew indicates a need to investigate data points with lower residuals. While no clear patterns emerge in the "versus fits" plot with the current data, a more extensive analysis could uncover systematic trends requiring additional independent variables or exploring non-linear relationships.

Finally, the "versus order" plot warrants further investigation with more data points to monitor for temporal dependencies. Overall, these analyses provide valuable insights for further model development.

An examination of **Fig.7-a** and **7-b** suggests that Vol% exerts a stronger individual influence on strain compared to the interaction effect. However, within the interaction plot, the lowest mesh size appears to exhibit the greatest strain response at the 20% Vol% level.

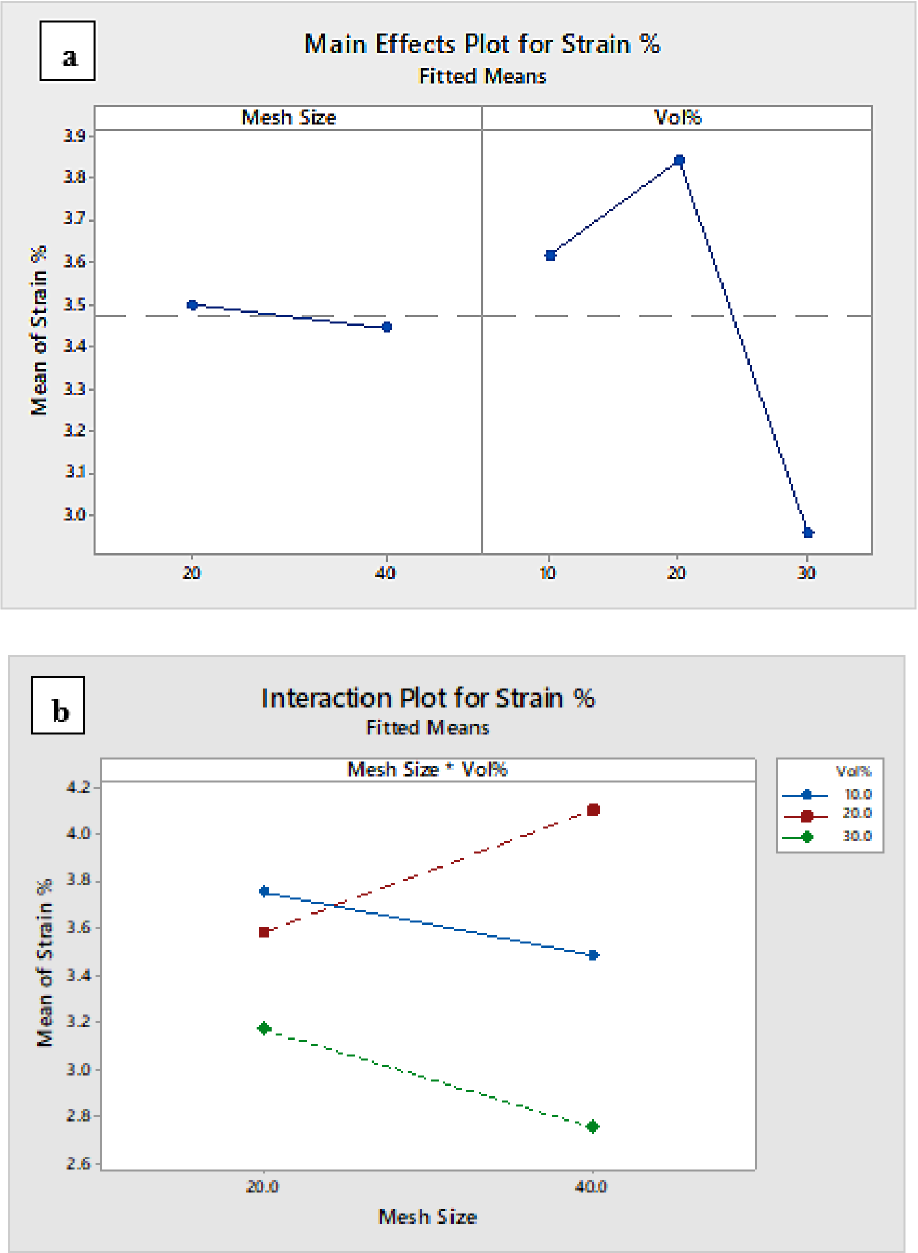

Fig. 7: (a) Main effects plot for strain, (b) Interaction plot for strain.

4.4. Analysis of impact resistance

The ANOVA analysis of the impact resistance of the manufactured composites is tabulated in **Table 6**. The model demonstrates a statistically significant effect on the response variable (p-value = 0). This suggests that one or more of the investigated factors (mesh size, Vol%, or their interaction) exert a statistically meaningful influence on the response variable. The highly significant value of the F-value further strengthens this conclusion, indicating that the model explains that vol% has the highest influence.

Table 6. ANOVA of impact resistance.

Analysis of Variance					
Source	DF	Adj SS	Adj MS	F-Value	P-Value
Model	5	109.296	21.859	18.7	0
Linear	3	71.834	23.945	20.48	0
Mesh Size	1	5.559	5.559	4.76	0.05
Vol%	2	66.275	33.137	28.34	0
2-Way Interactions	2	37.462	18.731	16.02	0
Mesh Size*Vol%	2	37.462	18.731	16.02	0
Error	12	14.03	1.169		
Total	17	123.326			

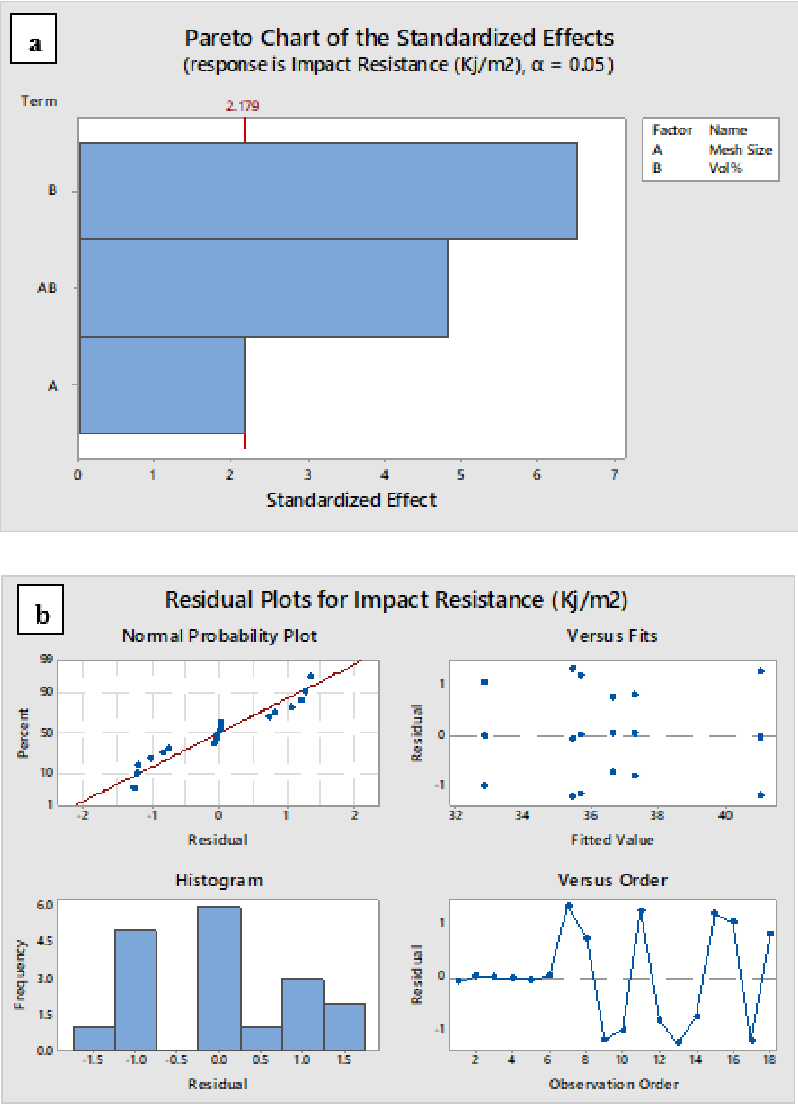

Fig. 8: (a) Pareto chart of impact resistance, (b) Residual plots for impact resistance.

The Pareto chart in **Fig. 8-a** suggests that Factor B (Vol %) and the interaction between Factor A (mesh size) and Factor B (Vol %) are the most important factors affecting impact resistance. These factors should be prioritized for further investigation or optimization. The normality plot reveals deviations from a perfect normal distribution, particularly in the tails (**Fig. 8-b**). This suggests potential non-normality in the residuals. Encouragingly, the versus plot in the same figure exhibits no discernible trends. This absence of patterns indicates no apparent relationship between the order of data collection and the magnitude of the residuals.

Consistent with the findings for strain, **Fig. 9-a** and **9-b** reveal that Vol% and its interaction with mesh size exert the strongest influence on impact resistance. **Fig. 9-a** further suggests that the effect of Vol% variation on impact resistance is more pronounced at smaller mesh sizes.

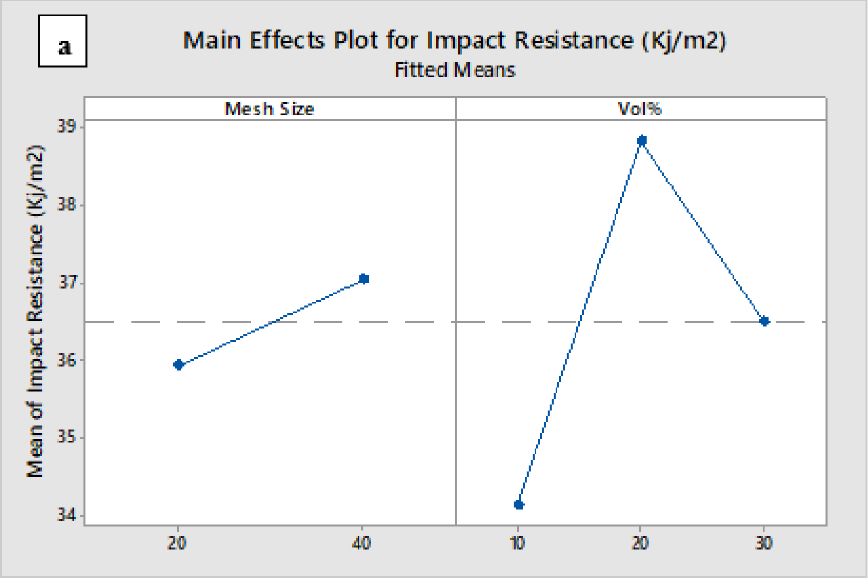

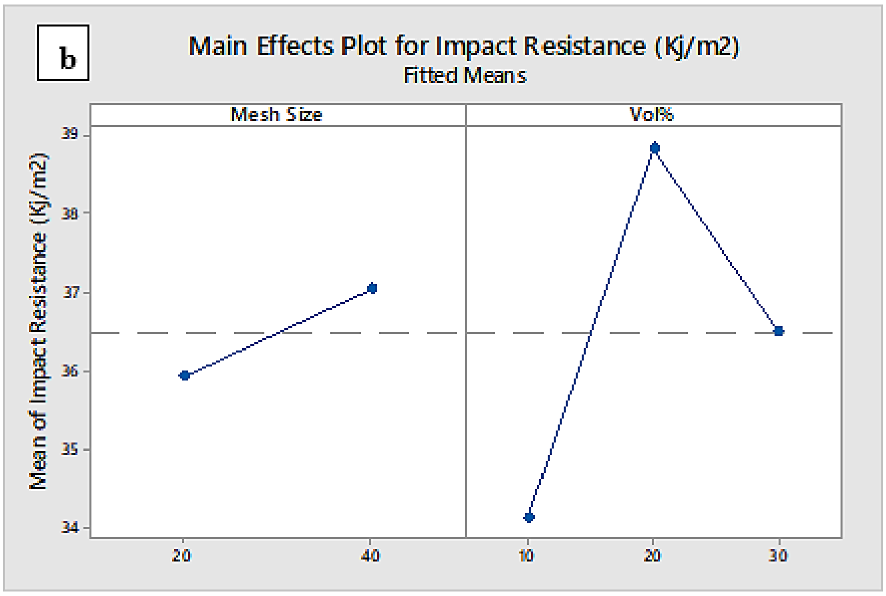

Fig. 9: (a) Main effects plot for impact resistance, (b) Interaction plot for impact resistance.

4.5. Analysis of Natural Frequency

The results presented in **Table 7** demonstrate a statistically significant effect of the model on the response variable (p-value < 0.05). This significance is further bolstered by the exceptionally low p-value (0.000), suggesting a robust association between the model and the response variable. However, focus on the F-value, despite its high values, may not pinpoint the specific factor driving this difference, however, the preference is for the mesh size.

Table 7: ANOVA of natural frequency.

Analysis of Variance					
Source	DF	Adj SS	Adj MS	F-Value	P-Value
Model	5	3002.28	600.46	150.11	0
Linear	3	2719.94	906.65	226.66	0
Mesh Size	1	1104.5	1104.5	276.12	0
Vol%	2	1615.44	807.72	201.93	0
2-Way Interactions	2	282.33	141.17	35.29	0
Mesh Size*Vol%	2	282.33	141.17	35.29	0
Error	12	48	4		
Total	17	3050.28			

Fig. 10-a presents the results to visualize each factor's relative importance. Examining the figure, we can observe that the interaction between Mesh Size and Vol% appears to have the weakest influence among the investigated factors.

Fig. 10-b utilizes graphical tools to assess the normality and independence of the residuals. The normality plot suggests a potential for normality in the residuals, with the data points lying close to the ideal straight line. This distribution pattern is indicative of a normal distribution.

For a more in-depth analysis, incorporate a histogram depicting the distribution of the residuals. Ideally, a bell-shaped curve centered around zero would signify normality. While the histogram may exhibit some asymmetry, it is crucial to consider it in conjunction with the normality plot for a more comprehensive evaluation.

The scatter plot depicted in **Fig. 10-b** is reassuring, as it exhibits no concerning trends or discernible patterns. This absence of trends suggests a lack of significant association between the data collection order and the residual values' magnitude.

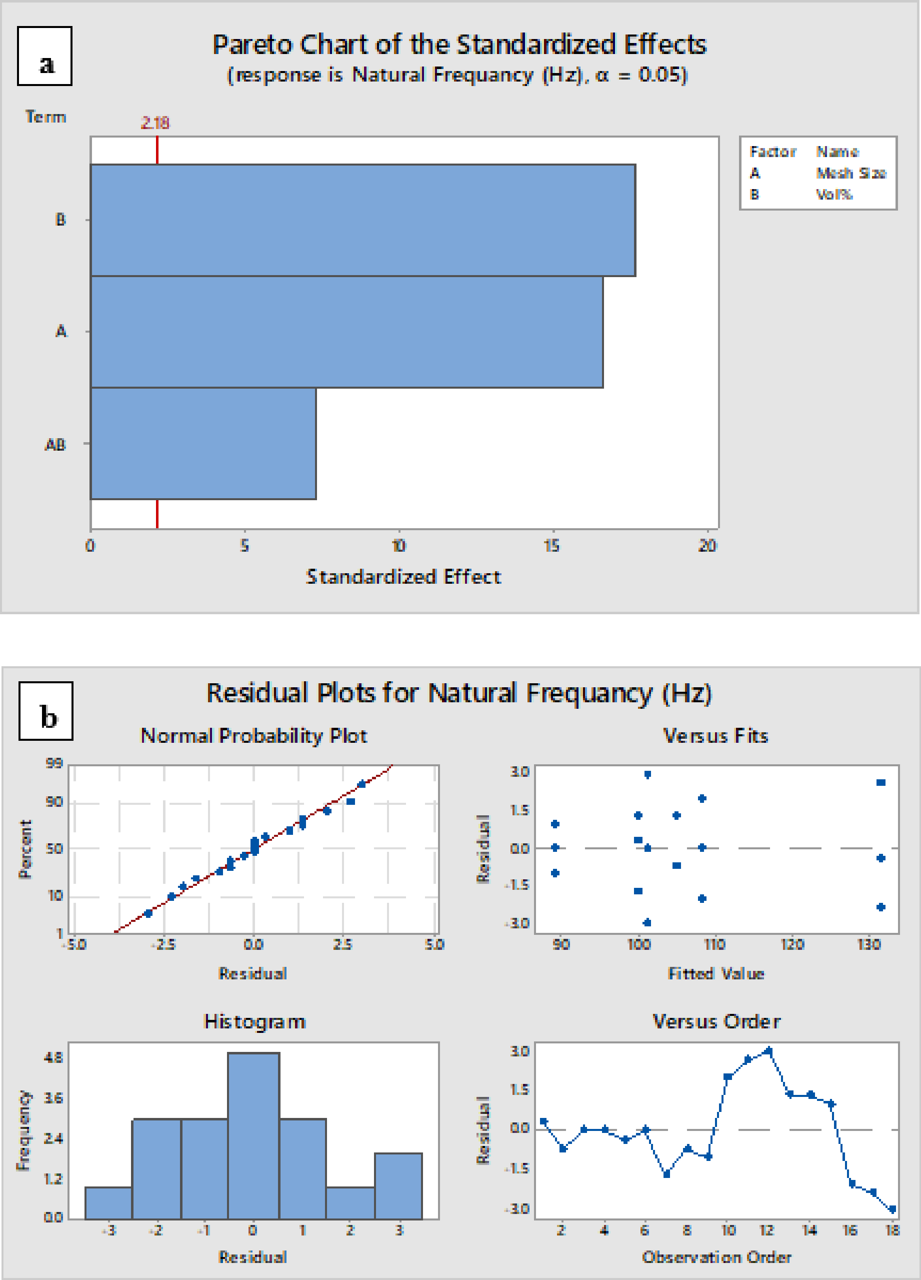

Fig. 10: (a) Pareto chart of natural frequency, (b) Residual plots for natural frequency.

Furthermore, the final analysis graphs in **Fig. 11-a** and **11-b** point toward the volume percentage having more influence, and an optimal configuration at a mesh size of 40 and a concentration of 20%.

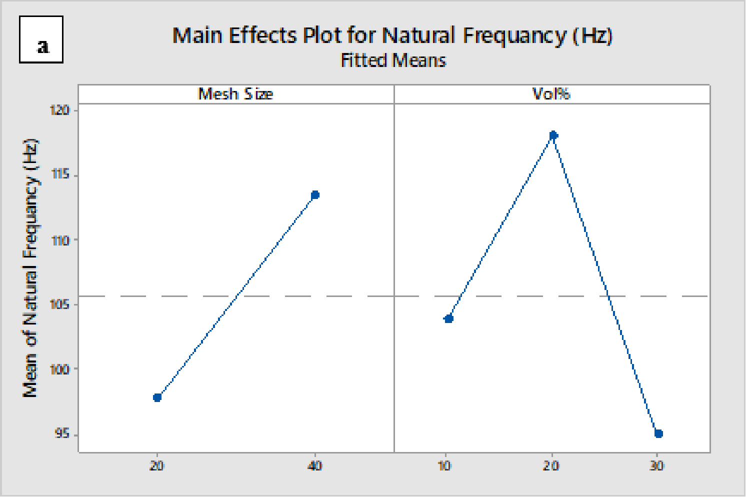

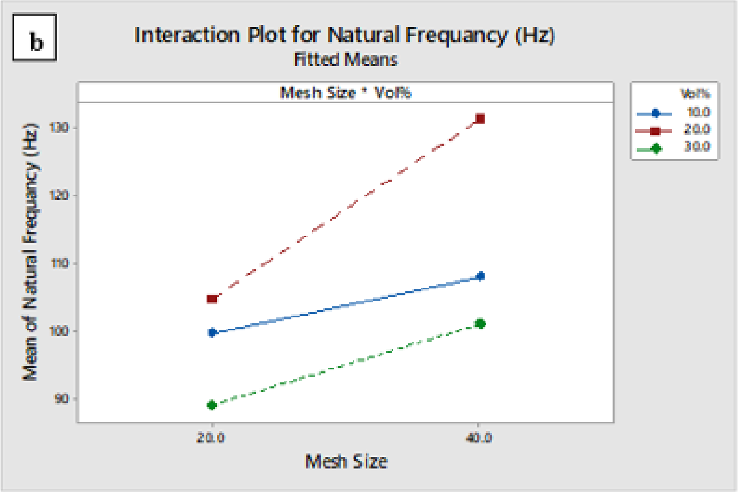

Fig. 11: (a) Main effects plot for natural frequency, (b) Interaction plot for natural frequency.

4.6. Analysis of Damping Ratio

The analysis of variance (ANOVA) results in **Table 8** reveals a statistically important mathematical model for explaining the observed trends. Independently, mesh size has a statistically significant effect (p=0.002, F=15.99) on the response variable, which is confirmed in the Pareto chart in **Fig. 12-a**.

Table 8: ANOVA of damping ratio.

Analysis of Variance					
Source	DF	Adj SS	Adj MS	F-Value	P-Value
Model	5	0.0042	0.00084	4.75	0.013
Linear	3	0.00367	0.00122	6.92	0.006
Mesh Size	1	0.00283	0.00283	15.99	0.002
Vol%	2	0.00084	0.00042	2.38	0.135
2-Way Interactions	2	0.00053	0.00026	1.49	0.265
Mesh Size*Vol%	2	0.00053	0.00026	1.49	0.265
Error	12	0.00212	0.00018		
Total	17	0.00632			

To identify the factors with the greatest influence on this effect, **Fig. 12-a** offers insights into their relative importance. Notably, the interaction term between Mesh Size and Vol% appears to be the most impactful factor.

Fig. 12-b presents a residual analysis to assess the normality and independence of the residuals. The normality plot in this figure suggests that the residuals may be reasonably close to a normal distribution, as evidenced by their distribution close to a straight line.

Complementing the normality plot, the histogram in **Fig. 12-b** depicts the distribution of the residuals. Ideally, a bell-shaped curve centered around zero would indicate perfect normality. Although the histogram may not be perfectly symmetrical, it should be considered alongside the normality plot for a more comprehensive evaluation of the normality assumption.

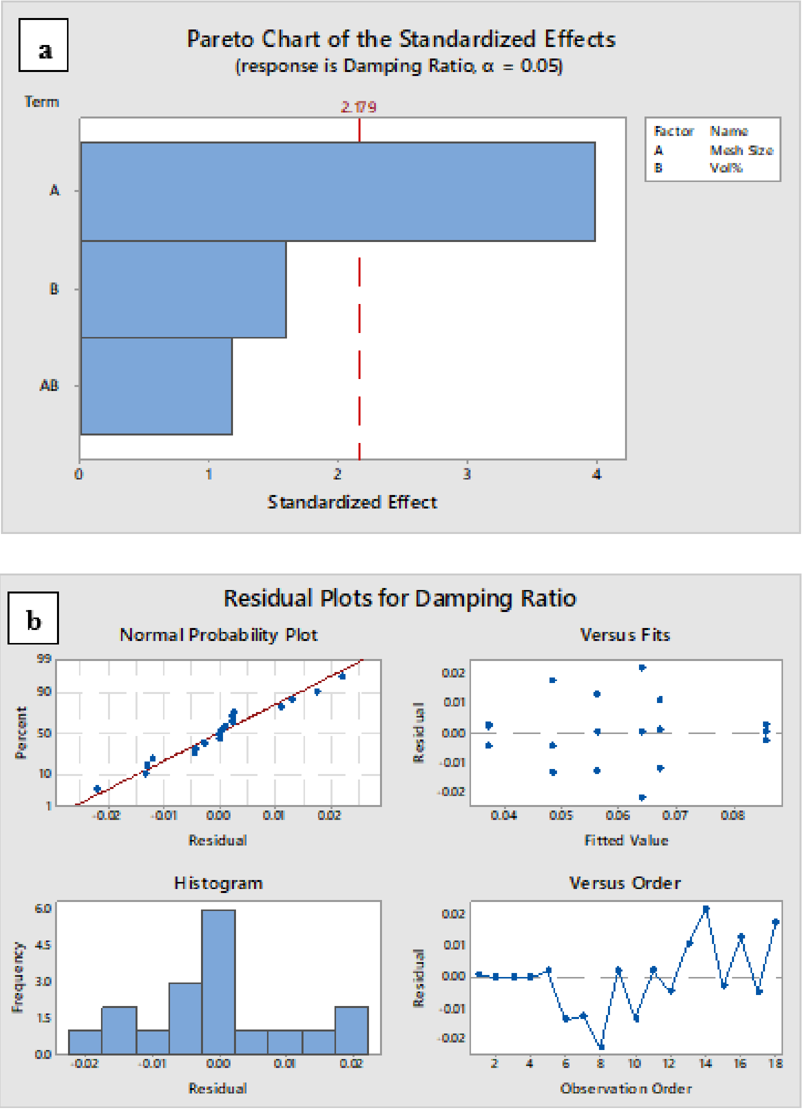

Fig. 12: (a) Pareto chart of damping ratio, (b) Residual plots for damping ratio.

The residuals in the versus plot (**Fig. 12-b**) are reassuring. The absence of any discernible trends or patterns suggests a lack of correlation between the order of data collection and the magnitude of the residuals. This characteristic is desirable for ensuring the validity of subsequent analyses.

The main effects plot in **Fig. 13-a** for the damping ratio reveals a potential decrease in damping with an increase in mesh size, with a steeper decline observed at the lower Vol% value. However, without p-values from a statistical test, it's impossible to determine if these trends are statistically significant. In **Fig. 13-b** the interaction plot of the damping factor shows that optimism is 20 mesh at a high-volume percentage, which means the direct proportion between the damping factor with the investigated factors.

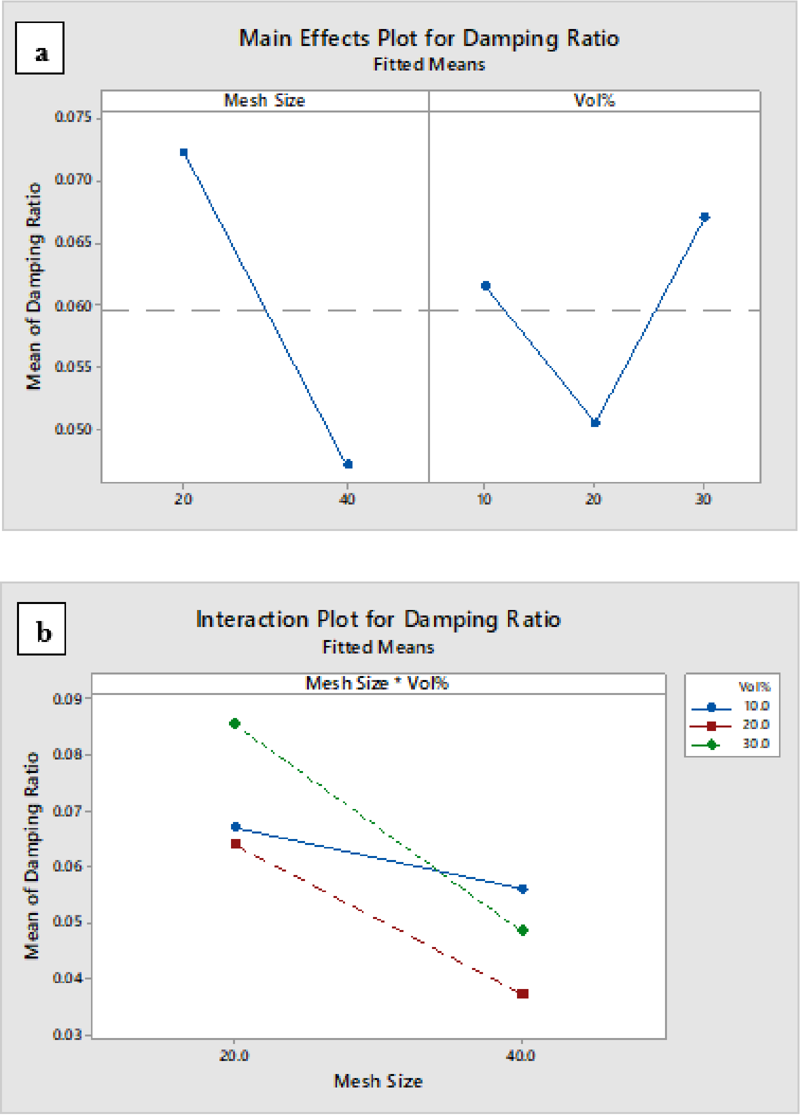

Fig. 13: (a) Main effects plot for damping ratio, (b) Interaction plot for damping ratio.

Conclusions

The Conclusions based on the factorial design analysis:

Ultimate Tensile Strength (UTS): Both mesh size and its interaction with rubber volume fraction significantly affect UTS. Finer mesh sizes (higher mesh number) generally lead to higher UTS. In contrast, the positive effect of finer mesh can be mitigated or reversed at higher rubber content (30%) due to opposing trends.

Strain: Rubber volume fraction and its interaction with mesh size strongly influence strain. The effect of volume fraction is stronger than the interaction effect. A lower mesh size with a 20% rubber volume fraction shows the greatest strain response.

Impact Resistance: Mesh size interaction with rubber volume fraction is the most important factor, the effect of volume fraction is more pronounced at smaller mesh sizes. There might be an optimal balance between rubber content and mesh size for maximizing impact resistance.

Natural Frequency: The interaction between mesh size and volume fraction has the weakest influence on natural frequency. Rubber content has a stronger influence, with higher content leading to lower natural frequency due to increased elasticity.

Damping Factor: Mesh size has a significant effect, with a potential decrease in damping with increasing mesh size. The interaction between mesh size and volume fraction might be the most impactful factor, although further investigation is needed, an optimal configuration of mesh size and rubber content (20 mesh at a high-volume percentage) for maximizing damping.

These conclusions highlight the importance of considering both mesh size and rubber volume fraction when designing composites for specific mechanical properties. The factorial design effectively captured the interaction effects between these factors, providing valuable insights for optimization.

For future work, more variables must be studied with more particle sizes and volume percentages to optimize the rubber addition also the types of fiberglass and laminate configurations should be investigated to reach the optimum design of this novel composite with integrated properties.

ACKNOWLEDGMENTS

The authors wish to acknowledge the effort and support of Dr. Essam Bahgat at King Abdulaziz University Faculty of Engineering in KSA, for his contributions.

References

[1] L. Banasiak, G. Chiaro, A. Palermo, and G. Granello, "Environmental Implications of the Recycling of End-of-Life Tires in Seismic Isolation Foundation Systems," Lect. Notes Civ. Eng., vol. 144 LNCE, pp. 43–52, 2021, doi: 10.1007/978-981-16-0077-7_5.

[2] N. F. Medina, R. Garcia, I. Hajirasouliha, K. Pilakoutas, M. Guadagnini, and S. Raffoul, "Composites with recycled rubber aggregates: Properties and opportunities in construction," Constr. Build. Mater., vol. 188, pp. 884–897, Nov. 2018, doi: 10.1016/J.CONBUILDMAT.2018.08.069.

[3] M. Mosaad, I. Mousa, S. S. Mohamed, and M. Academy, "Drilling Performance Evaluation of Innovative Waste Tire Rubber-Reinforced Polyester-Fiberglass Laminated Composites," vol. 2024, no. 9, pp. 105–112, 2024.

[4] M. S. EL-Wazery, M. I. EL-Elamy, and S. H. Zoalfakar, "Mechanical properties of glass fiber reinforced polyester composites," Int. J. Appl. Sci. Eng., vol. 14, no. 3, pp. 121–131, 2017, doi: 10.6703/IJASE.2017.14(3).121.

[5] H. H. Parikh and P. P. Gohil, "Experimental determination of tribo behavior of fiber-reinforced composites and its prediction with artificial neural networks," Durab. Life Predict. Biocomposites, Fibre-Reinforced Compos. Hybrid Compos., pp. 301–320, Jan. 2018, doi: 10.1016/B978-0-08-102290-0.00013-1.

[6] N. Botha, H. M. Inglis, R. Coetzer, and W. J. L. F. Johan, "Statistical Design of Experiments: An introductory case study for polymer composites manufacturing applications," 12th South African Conf. Comput. Appl. Mech. SACAM 2020, 2020, doi: 10.1051/MATECCONF/202134700028.

[7] D. D. Vineta Srebrenkoska and Gordana Bogoeva Gaceva, "Application of Factorial Experimental Design in Predicting Mechanical Properties of Polypropylene based Composites," Int. J. Eng. Res. Technol., vol. 5, no. 2, pp. 96–98, 2016, [Online]. Available: http://www.ijert.org

[8] L. Feng, R. Li, H. Yang, S. Chen, and W. Yang, "The Hyperbranched Polyester Reinforced Unsaturated Polyester Resin," Polymers (Basel)., vol. 14, no. 6, Mar. 2022, doi: 10.3390/POLYM14061127.

[9] S. Vishnu, B. Prabu, and M. Pugazhvadivu, "Strategies to improve the mechanical performance of elastomers using ternary blends: A review," Hybrid Adv., vol. 3, p. 100062, Aug. 2023, doi: 10.1016/J.HYBADV.2023.100062.

[10] "HOPPEC | HOPPEC SBR 0.0 mm – 0.8mm Powder Rubber." Accessed: Jul. 01, 2024. [Online]. Available: https://www.hoppec.net/en/singleProduct/40/HOPPEC_SBR_0.0_mm_–_0.8mm_Powder_Rubber

[11] "Fiberglass Mats and Woven Rovings_Product Description_PRODUCT&SERVICE_China Jushi Co., Ltd." Accessed: Jun. 30, 2024. [Online]. Available: https://www.jushi.com/en/product/product-introduction-145.html

[12] S. W. Ghori, R. Siakeng, M. Rasheed, N. Saba, and M. Jawaid, "The role of advanced polymer materials in aerospace," Sustain. Compos. Aerosp. Appl., pp. 19–34, Jan. 2018, doi: 10.1016/B978-0-08-102131-6.00002-5.

[13] A. S.Abdel-Wanees, B. Hany Mousa, I. M.Ibrahim, and T. S.Mahmoud, “Assessment Study on the Mechanical Behavior of Polyester – Fiber Composite Laminates Filled with Waste Tire Rubber Particles,” Benha J. Appl. Sci., vol. 7, no. 4, pp. 21–23, 2022, doi: 10.21608/bjas.2022.251248.

[14] M. Mosaad, T. S.Mahmoud, B. Hany Mousa, I. Mousa, and S. S. Mohamed, “Investigation On the Effect of Variation of Drilling Parameters On the Delamination Factor in Waste Tire Rubber Polyester Composite Laminates,” Benha J. Appl. Sci., vol. 7, no. 4, pp. 249–252, 2022, doi: 10.21608/bjas.2022.260500.

[15] ASTM Committee D30, “D3039/D3039M: Standard Test Method for Tensile Properties of Polymer Matrix Composite Materials,” Annu. B. ASTM Stand., vol. 15, pp. 1–13, 2017, [Online]. Available: http://scholar.google.com/scholar?hl=en&btnG=Search&q=intitle:Standard+Test+Method+for+Tensile+Properties+of+Polymer+Matrix+Composite+Materials#1

[16] S. T. Method, “iTeh Standards iTeh Standards Document Preview,” vol. 08, no. Reapproved 1989, pp. 3–4, 2000.

[17] V. N. Paimushin, V. A. Firsov, V. M. Shishkin, V. A. Kostin, and R. S. Gimadiev, “Erratum to: An Investigation into the ASTM E756-05 Test Standard Accuracy on Determining the Damping Properties of Materials in Tension-Compression (Russian Aeronautics, (2020), 63, 2, (205-213), 10.3103/S106879982002004X),” Russ. Aeronaut., vol. 63, no. 3, p. 547, Sep. 2020, doi: 10.3103/S1068799820030277.

[18] K. Fathy, A. Elenien, A. Abdel-wahab, R. Elgamsy, and M. H. Abdellatif, “Assessment of the properties of PP composite with addition of recycled tire rubber Assessment of the properties of PP composite with addition of recycled tire rubber,” Ain Shams Eng. J., vol. 9, no. 4, pp. 3271–3276, 2018, doi: 10.1016/j.asej.2018.05.001.

[19] B. H. Mousa, R. El Gamsy, and M. H. A. Latif, “Mechanical behaviour of rubber hybrid composites,” Int. Conf. Aerosp. Sci. Aviat. Technol., vol. 18, no. 18, pp. 1–8, Apr. 2019, doi: 10.1088/1757-899X/610/1/012064.

[20] A. S. A. Wanees, T. S. Mahmoud, I. M. Ibrahim, and A. O. Mosleh, “Development of Eco - Friendly Composites : Lamination Configuration and Addition of Waste Tire Rubber Particles on the Mechanical Performance of Polyester - Fiberglass Composite Plates,” vol. 2024, no. 9, pp. 69–79, 2024.

[21] A. Treviso, B. Van Genechten, D. Mundo, and M. Tournour, “Damping in composite materials: Properties and models,” Compos. Part B Eng., vol. 78, pp. 144–152, Aug. 2015, doi: 10.1016/J.COMPOSITESB.2015.03.081.

[22] A. Jahan, K. L. Edwards, and M. Bahraminasab, “Multiple objective decision-making for material and geometry design,” Multi-criteria Decis. Anal. Support. Sel. Eng. Mater. Prod. Des., pp. 127–146, 2016, doi: 10.1016/B978-0-08-100536-1.00006-0.

[23] H. R. E. H. Bouchekara, G. Dahman, and M. Nahas, “Smart electromagnetic simulations: Guidelines for design of experiments technique,” Prog. Electromagn. Res. B, no. 31, pp. 357–379, 2011, doi: 10.2528/PIERB11052104.

[24] M. D. G. Ambrosio et al., “A Factorial Randomized Controlled Trial to Optimize User Engagement With a Chatbot-Led Parenting Intervention: Protocol for the ParentText Optimisation Trial,” JMIR Res. Protoc., vol. 13, 2024, doi: 10.2196/52145.